

Supporting Information

Over 19.2% efficiency of layer-by-layer organic photovoltaics enabled by highly crystalline material as energy donor and nucleating agent

Hongyue Tian^a, Yuheng Ni^a, Wenqing Zhang^b, Yujie Xu^b, Bing Zheng^c, Sang Young Jeong^d, Sijian Wu^e, Zaifei Ma^e, Xiaoyan Du^b, Xiaotao Hao^b, Han Young Woo^{d*}, Lijun Huo^f, Xiaoling Ma^{a,g*} and Fujun Zhang^{a,g*}

^a Key Laboratory of Luminescence and Optical Information, Ministry of Education, Beijing Jiaotong University, Beijing, 100044, P. R. China.

^b School of Physics, State Key Laboratory of Crystal Materials, Shandong University, Jinan, Shandong, 250100, P. R. China.

^c School of Pharmacy, Shandong Second Medical University, Weifang, Shandong, 261053, P. R. China.

^d Organic Optoelectronic Materials Laboratory, Department of Chemistry, College of Science, Korea University, 02841, Seoul, Republic of Korea.

^e State Key Laboratory for Modification of Chemical Fibers and Polymer Materials, Center for Advanced Low-dimension Materials, College of Materials Science and Engineering, Donghua University, Shanghai, 201620, P. R. China.

^f School of Chemistry, Beihang University, Beijing 100191, P. R. China.

^g Tangshan Research Institute of Beijing Jiaotong University, Tangshan, 063000, P. R. China.

*Correspondence: hywoo@korea.ac.kr, xlma2@bjtu.edu.cn and fjzhang@bjtu.edu.cn.

Experimental section

Device Fabrication

The patterned indium tin oxide (ITO) coated glass substrates (15 Ω per square) were cleaned via sequential sonication in detergent, de-ionized and ethanol and then blow-dried by high-purity nitrogen. All pre-cleaned ITO substrates were treated by oxygen plasma for 1 minute (min) to improve their work function and clearance. Then, the poly(3,4-ethylenedioxythiophene): poly(styrene sulfonate) (PEDOT:PSS, purchased from H.C. Starck co. Ltd.) solution was spin-coated on ITO substrates at 5000 round per minute (rpm) for 40 s and dried at 150 °C for 15 min in atmospheric air. Then ITO substrates coated with PEDOT:

PSS films were transferred into a high-purity nitrogen-filled glove box. The polymer donor PM1 and small molecule acceptor L8-BO were purchased from Solarmer Materials Inc. The PM1:D18A with different mass ratios (1:0, 1:0.15, 1:0.3, 1:0.5, 1:1) were dissolved in chloroform to prepare the blend donor solutions. The acceptor L8-BO was dissolved in chloroform to prepare the acceptor solutions with the concentration of 8 mg/ml, and 10 mg/ml TCB was added as an additive. The donor layer was spin coated from donor solutions on top of the PEDOT: PSS layer, the donor layers were thermal annealed at 80 °C for 8 min. The acceptor layer was spin coated from acceptor solutions at 2700 rpm for 40 s on the top of the donor layer. Then, the whole active layers were thermally annealed at 100 °C for 5 min. PNDIT-F3N was purchased from eflex PV limited company. The PNDIT-F3N was dissolved in methanol with the addition of 0.25 vol% acetic acid to prepare a 0.5 mg/ml solution. The prepared PNDIT-F3N solution was spin-coated onto the active layers at 2000 rpm for 30 s. Finally, 100 nm Ag was deposited by thermal evaporation. The active area is approximately 3.8 mm², defined by the overlapping area of ITO anode and Ag cathode.

Devices Measurement

The current-voltage (J - V) curves of LbL OPVs were measured in a high-purity nitrogen-filled glove box using a Keithley 2400 source meter. AM 1.5G irradiation at 100 mW cm⁻² was provided by an XES-40S2 (SAN-EI Electric Co., Ltd.) solar simulator (AAA grade, 70×70 mm² photobeam size), which was calibrated by standard monocrystalline silicon reference solar cells. The external quantum efficiency (EQE) spectra of OPVs were measured in air conditions by a Zolix Solar Cell Scan 100. The absorption spectra of films were measured with a Shimadzu UV-3101 PC spectrometer. Photoluminescence (PL) spectra of films were measured by a HORIBA Fluorolog®-3 spectrofluorometer system.

Transient photovoltage (TPV) and transient photocurrent (TPC) were conducted with the Parioscarrier measurement system (FLUXiM AG, Switzerland). A high-power white LED is utilized as light source for TPV and TPC. The integrated power of the LED is 72mW cm⁻², and the spectrum distribution is mainly in the wavelength range of 440-470 nm and 540-630 nm, and the peak value located at 460 nm and 550 nm. Electrochemical impedance spectroscopy was measured by a ZAHNER CIMPS electrochemical workstation, Germany. Grazing incidence wide angle X-ray scattering (GIWAXS) measurements were accomplished at PLS-

II 9A U-SAXS beamline of the Pohang Accelerator Laboratory in Korea.

The contact angle images were obtained using a surface contact angle tester (Zhongchen, JC2000D1, China). The contact angles of neat PM1, D18A, and L8-BO films and PM1:D18A blend films were measured based on H₂O and CH₂I₂. The surface energy of films was calculated according to the contact angles by using Wu's model. According to the surface energy of films, the interfacial energy between various films can be evaluated by the following equation (1):

$$\gamma_{AB} = \gamma_A + \gamma_B - \frac{4\gamma_A^d \gamma_B^d}{\gamma_A^d + \gamma_B^d} - \frac{4\gamma_A^p \gamma_B^p}{\gamma_A^p + \gamma_B^p} \quad (1)$$

Here, γ_{AB} is the interfacial energy between material A and B; γ_A and γ_B are the surface energy of the pure materials; superscript d and p represent the dispersion and polar components calculated by using the contact angles.

The energy loss (E_{loss}) of typical LbL OPVs were investigated. V_{OC}^{rad} is the voltage of radiative limit, which can be obtained according to the following equation:

$$V_{OC}^{rad} = \frac{kT}{q} \ln \left(\frac{J_{SC}}{J_0^{rad}} + 1 \right) \cong \frac{kT}{q} \ln \left(\frac{q \cdot \int_0^{+\infty} EQE_{PV}(E) \cdot \phi_{AM\ 1.5G}(E) \cdot dE}{q \cdot \int_0^{+\infty} EQE_{PV}(E) \cdot \phi_{BB}(E) \cdot dE} \right) \quad (2)$$

Here, k , T , and q represent the Boltzmann constant, temperature of samples, and elementary charge, separately. J_0^{rad} is the saturation current density calculated by considering only the blackbody radiation of the real absorption profile.

The photogenerated current density (J_{ph}) versus effective voltage (V_{eff}) characteristic was measured in a high-purity nitrogen-filled glove box. The J_{ph} is represented as $J_L - J_D$, where J_L and J_D represent the current densities under one-sun illuminated and dark conditions, separately. The V_{eff} is represented as $V_0 - V_a$, in which V_0 and V_a represent the voltage at $J_{ph} = 0$ mA cm⁻² and applied voltage, separately. The J_{ph} can be defined as saturated photocurrent density (J_{sat}) at the relatively large V_{eff} , in which situation all the photogenerated excitons are assumed to be dissociated into free carriers and then be collected by the electrodes.

The structure of sole-electron devices is ITO/ZnO/active layer/PNDIT-F3N/Al and the

structure of sole-hole devices is ITO/PEDOT: PSS/active layer/MoO₃/Ag. The fabrication conditions of the active layer films are same with those for the OPVs. The charge mobilities are generally described by the Mott-Gurney equation (2):

$$J = \frac{9}{8} \varepsilon_r \varepsilon_0 \mu \frac{V^2}{L^3} \quad (3)$$

where J is the current density, ε_0 is the permittivity of free space (8.85×10^{-14} F/cm), ε_r is the dielectric constant of used materials, μ is the charge mobility, V is the applied voltage and L is the active layer thickness. The ε_r parameter is assumed to be 3 as a typical value for organic materials. In organic materials, charge mobility is usually field dependent and can be described by the disorder formalism, typically varying with electric field, $E=V/L$, according to the equation (3):

$$\mu = \mu_0 \exp\left[0.89\gamma \sqrt{\frac{V}{L}}\right] \quad (4)$$

where μ_0 is the charge mobility at zero electric field and γ is a constant. Then, the Mott-Gurney equation can be described by (4):

$$J = \frac{9}{8} \varepsilon_r \varepsilon_0 \mu_0 \frac{V^2}{L^3} \exp\left[0.89\gamma \sqrt{\frac{V}{L}}\right] \quad (5)$$

In this case, the charge mobilities were estimated using the following equation (5):

$$\ln\left(\frac{JL^3}{V^2}\right) = 0.89\gamma \sqrt{\frac{V}{L}} + \ln\left(\frac{9}{8} \varepsilon_r \varepsilon_0 \mu_0\right) \quad (6)$$

Additional experimental results

Table S1. Contact angles, surface energy (γ), dispersion (γ^d) and polar (γ^p) components of individual films, and interfacial energy ($\gamma_{X/Y}$) between two films.

Film (X)	Contact angle H ₂ O (deg)	Contact angle CH ₂ I ₂ (deg)	γ (mN m ⁻¹)	γ^d (mN m ⁻¹)	γ^p (mN m ⁻¹)	Film (Y)	$\gamma_{X/Y}$ (mN m ⁻¹)
PM1	95.51	43.62	31.89	30.85	1.03	L8-BO	1.92
D18A	79.74	44.09	33.47	26.51	6.96	L8-BO	8.89
PM1:D18A (1:0.3)	94.40	48.14	29.75	28.22	1.51	L8-BO	3.21
L8-BO	90.27	33.39	43.10	42.44	0.66	--	--

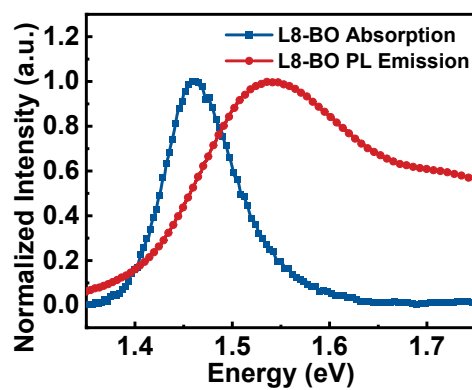


Figure S1. PL and absorption spectra for L8-BO film.

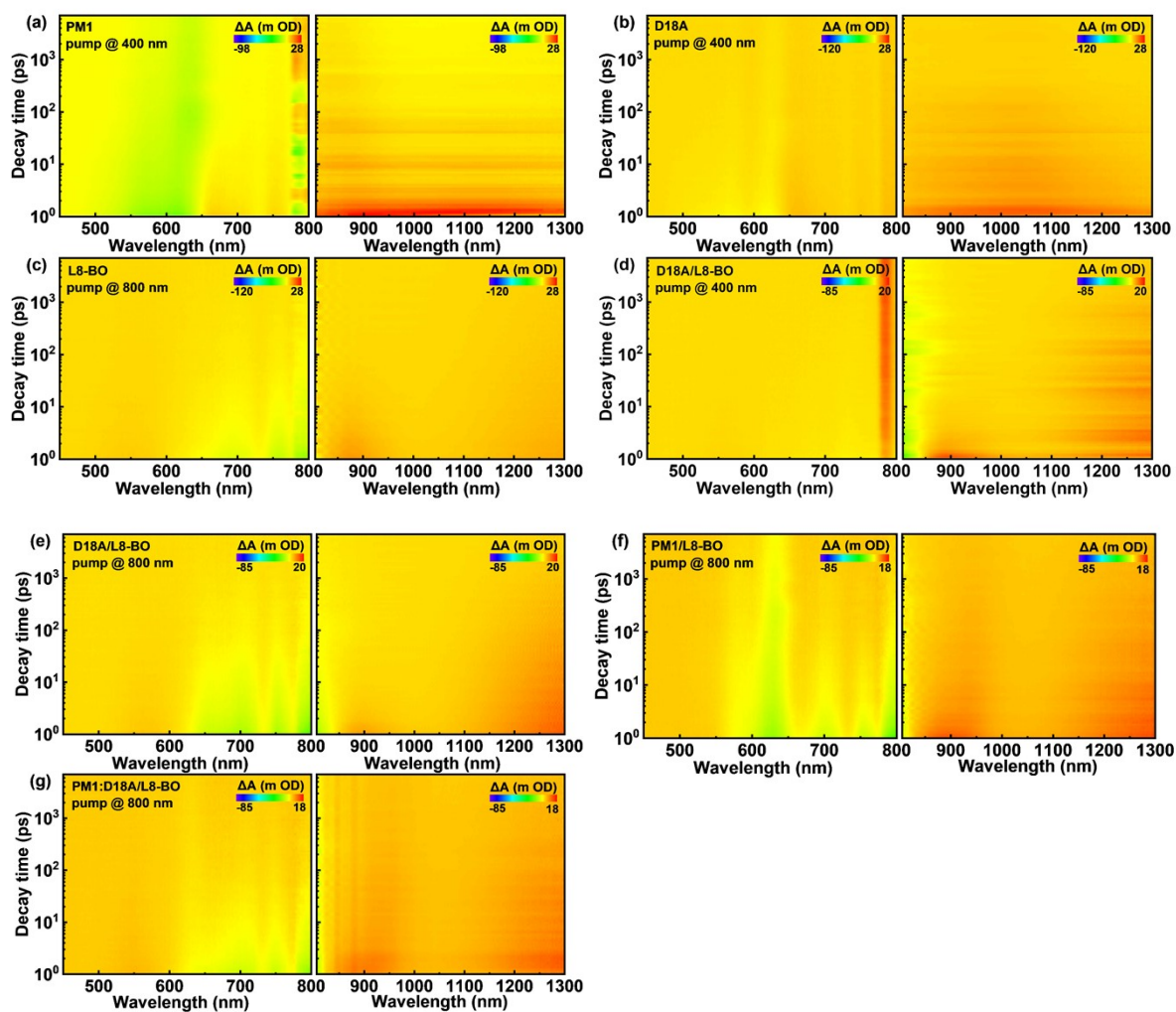


Figure S2. TA 2D plots of (a) neat PM1 and (b) D18A films pumped at 400 nm. TA 2D plots of (c) neat L8-BO films pumped at 800 nm, and (d) D18A/L8-BO LbL films pumped at 400 nm. TA 2D plots of (e) D18A/L8-BO, (f) PM1/L8-BO, (g) PM1:D18A/L8-BO LbL films pumped at 800 nm.

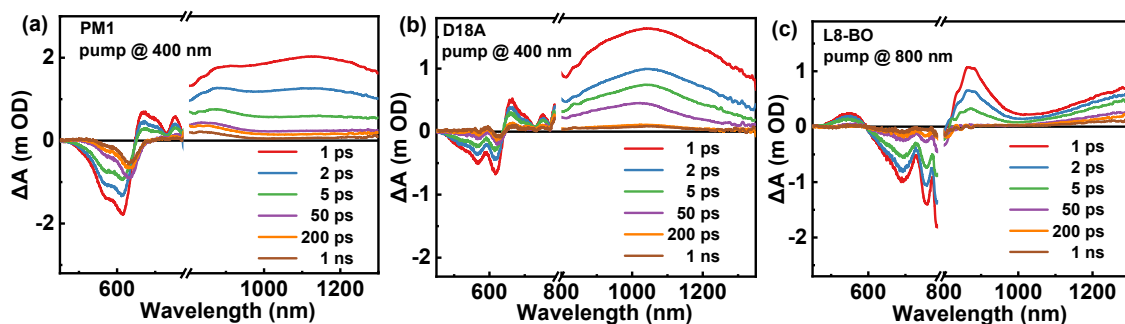


Figure S3. The TA spectra at different time delay of (a) PM1 films, and (b) D18A films pumped at 400 nm, (c) L8-BO films pumped at 800 nm.

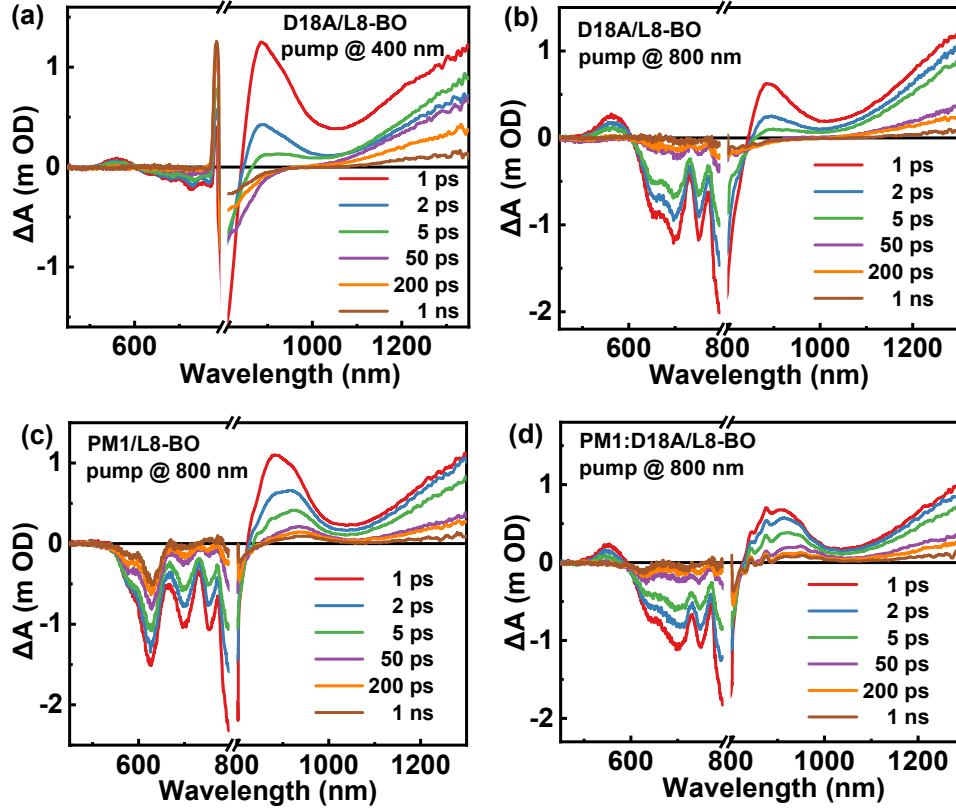


Figure S4. The TA spectra at different time delay of (a) D18A/L8-BO films pumped at 400 nm. (b) D18A/L8-BO films, (c) PM1/L8-BO, and (d) PM1:D18A/L8-BO films pumped at 800 nm.

Table S2. Device parameters obtained from J_{ph} - V_{eff} curves of LbL OPVs.

PM1:D18A	J_{ph}^* (mA cm ⁻²)	$J_{ph}^\#$ (mA cm ⁻²)	J_{sat} (mA cm ⁻²)	P_{diss} (%)	P_{coll} (%)
1:0	26.28	24.14	28.10	93.5	85.9
1:0.3	27.02	25.02	28.11	96.1	89.0
1:1	26.42	23.89	28.48	92.8	83.9

Table S3. The fitted parameters of LbL OPVs.

PM1:D18A	R_{OS} (Ω)	R_{CT} (Ω)	CPE-T (nF)	CEP-P
1:0	34.6	34.6	26.4	0.956
1:0.3	31.6	27.1	28.9	0.975
1:1	36.7	47.9	16.6	0.949

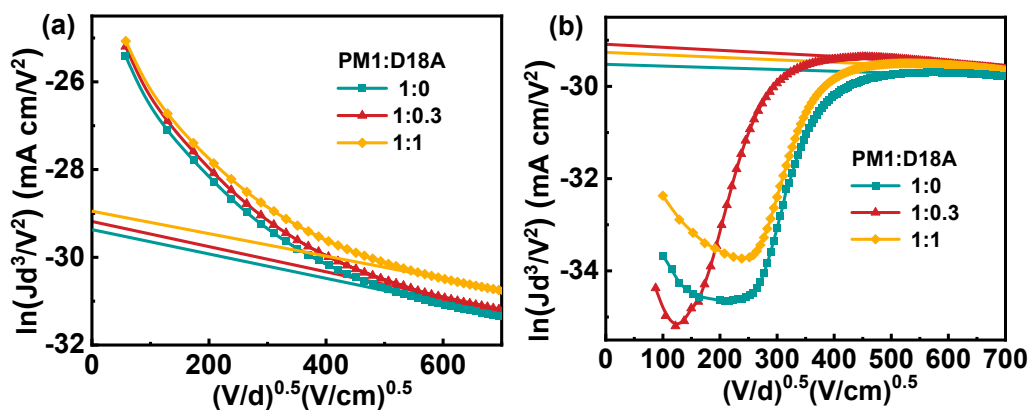


Figure S5. The $\ln(Jd^3/V^2)$ versus $(V/d)^{0.5}$ curves of (a) hole-only devices and (b) electron-only devices.

Table S4. The μ_h , μ_e and μ_h/μ_e values of layered films.

PM1:D18A	μ_h ($\text{cm}^2\text{V}^{-1}\text{s}^{-1}$)	μ_e ($\text{cm}^2\text{V}^{-1}\text{s}^{-1}$)	μ_h/μ_e
1:0	5.8×10^{-4}	4.9×10^{-4}	1.18
1:0.3	7.1×10^{-4}	6.5×10^{-4}	1.09
1:1	8.9×10^{-4}	7.7×10^{-4}	1.16

Table S5. The different vector (q) values of diffraction peaks and crystal coherence length (CCL) of layered films.

PM1:D18A	Diffraction vector (\AA^{-1})		Crystal correlation length (\AA)	
	IP (100)	OOP (010)	IP (CCL_{100})	OOP (CCL_{010})
1:0	0.30	1.70	64.45	20.00
1:0.3	0.31	1.71	65.34	21.38
1:1	0.32	1.72	71.22	24.43

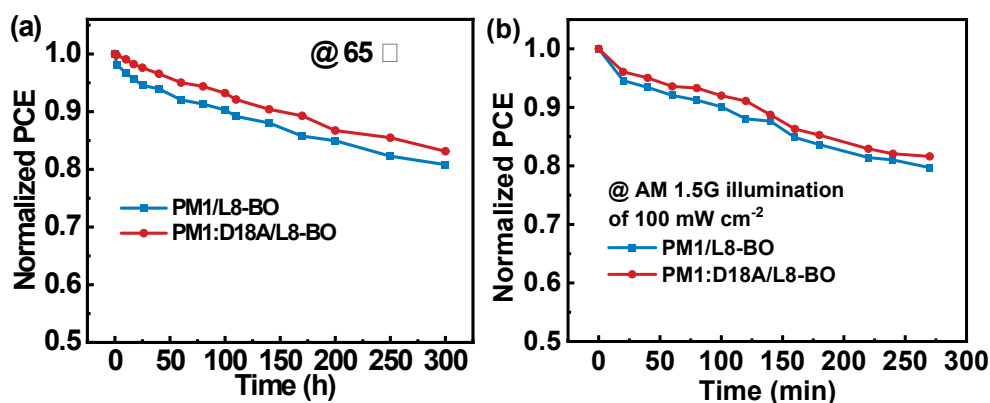


Figure S6. (a) PCE decay under 65 °C conditions, (b) PCE decay under AM 1.5G illumination of 100 mW cm⁻² condition.